Proton NMR Relaxation Study of Molecular Motions in a Liquid Crystal with a Strong Polar Terminal Group

P. J. Sebastião, A. C. Ribeiro

Centro de Física da Matéria Condensada (INIC)
Av. Prof. Gama Pinto 2, 1699 Lisboa Codex, Portugal

H. T. Nguyen

Centre de Recherche Paul Pascal, Avenue A. Schweitzer, 33600 Pessac Cedex, France

F. Noack

Physikalisches Institut der Universität Stuttgart, Pfaffenwaldring 57, 70550 Stuttgart, Germany

Z. Naturforsch. **48a**, 851–860 (1993); received April 22, 1993

Liquid crystalline compounds containing a cyano terminal group often exhibit peculiar molecular organizations of their mesophases. In this work we present proton NMR relaxation studies, performed by means of standard NMR and fast field-cycling NMR techniques, in the nematic (N) and bilayered smectic-*A* phase (S_{A2}) of 4-pentyl-phenyl 4′-cyanobenzoyloxy-benzoate. The field-cycling measurements were used to clarify the relaxation behaviour in the low Larmor frequency range, where conventional techniques are not applicable.

Self-diffusion and rotational reorientations are found to be the essential relaxation mechanisms at MHz frequencies in the smectic mesophase, while the contribution of collective modes appears only at lower frequencies in the kHz range. In the nematic mesophase the order director fluctuations mechanism dominates the relaxation dispersion up to 10 MHz, where the rotational reorientations become important, with minor corrections from the self-diffusion process. The agreement between the experimental findings and model fits could be improved by an additional relaxation mechanism in the kHz regime, ascribed to the interaction between protons and fast relaxing quadrupolar nitrogen ^{14}N nuclei. Though all four processes are present in the nematic and smectic-A_2 phases, the overall T_1 frequency dependence is quite different in the two cases. This behaviour is discussed in terms of available theoretical calculations of the proton relaxation dispersion in liquid crystals, and it is also compared with data known from other cyano compounds.

Key words: NMR; Proton relaxation; Smectic-A_2; Molecular motions; Bilayer smectic.

1. Introduction

Proton and deuteron NMR relaxation measurements have often been used to study molecular motions in liquid crystalline mesophases [e.g. 1, 2]. However, systematic Larmor frequency dependent studies, which allow to separate the underlying motional models more reliably than procedures at constant frequency, have only been performed for some simple nematic and smectic-*A* phases [3, 4], but not yet for systems with more special kinds of polymorphisms [5, 6] such as e.g. completely bilayered smectic phases and smectic antiphases or incommensurate phases.

Following previous preliminary work [7–9] on cyano liquid crystal compounds with a strong polar end group, we present here Larmor frequency dependent measurements of the longitudinal proton spin relaxation time T_1 ("relaxation dispersion") in the crystalline (C_r), nematic (N) and bilayered smectic-*A* (S_{A2}) phases of the liquid crystal 4-pentyl-phenyl 4′-cyanobenzoyloxy-benzoate

$$NC-\Phi-COO-\Phi-COO-\Phi-C_5H_{11},$$

which will be denoted by DB5CN. This material has an S_{A2} mesophase between 127 °C and 141 °C and a high-temperature N phase up to the clearing point at 256 °C [10]. The layer spacing in the bilayered smectic range is approximately twice the molecular length in the stretched conformation. Hardouin et al. [10] suggested a model based on the concept that molecules with strong polar heads arrange in head-to-head configuration, and thus entail bilayers with antiferroelectric order.

It is generally accepted that the proton spin relaxation of nematic and smectic liquid crystals reflects

Reprint requests to P. J. Sebastião, Av. Prof. Gama Pinto 2, 1699 Lisboa Codex, Portugal.

0932-0784 / 93 / 0800-0851 $ 01.30/0. – Please order a reprint rather than making your own copy.

both individual molecular reorientations (self-diffusion, rotations) and collective molecular fluctuations (order director fluctuations) [1–4, 7]. But the importance and separation of the three mechanisms is still heavily disputed in the literature, and as a consequence also most characteristic details of the models suggested for such superimposed relaxation rates have not been confirmed experimentally. For example, theoretically the translational self-diffusion process [11–13], the anisotropic rotational jumping [9, 14–17] and the collective mode spectrum [18–20] differ significantly between a nematic and smectic mesophase. However, the predicted distinctions have scarcely been observed so far by proton relaxation dispersion profiles of nematic and smectic-*A* liquid crystals [3, 4, 21, 22]. This rather surprising fact essentially initiated the present work on a compound exhibiting a nematic and bilayer smectic polymorphism, a system not yet studied in literature by NMR relaxation and where the expected changes could be more pronounced.

2. Experimental Techniques and Results

The longitudinal proton (spin-lattice) relaxation time T_1 of DB5CN was measured as a function of temperature (T) and Larmor frequency ($2\pi\nu$), by means of two different NMR techniques: For frequencies above 8 MHz, a commercial pulse spectrometer Bruker SXP-4/100 MHz and a Bruker CXP/300 MHz, with the standard T_1 pulse sequence ($\pi - \tau - \pi/2$), were used; between 100 Hz and 8 MHz the relaxation times were obtained by home-built fast field-cycling devices [3, 4, 23] and suitable pulse programs. All T_1 data were determined on cooling the sample from the nematic phase very slowly. In this way it was possible to orient the director field in the nematic phase. The temperature could be controlled within about $\pm 0.3\,°C$. Furthermore it was checked that the systematic deviations between the T_1 values obtained by the SXP and home-build spectrometers did not exceed the experimental error limits of $\pm 10\%$.

Figure 1 illustrates the temperature dependence of the proton T_1 in the crystalline, nematic and smectic-A_2 phases of DB5CN, at some selected frequencies ν. In any case T_1 increases with increasing temperature, as is well known from studies of familiar liquid crystals [1, 3, 4]. The $T_1(T)$ slope in the S_{A2} phase is almost identical to the one in the N phase, but it slightly decreases for smaller frequencies. At high ν's in the megahertz range, $T_1(T)$ is continuous for both the $Cr - S_{A2}$ and the $S_{A2} - N$ transitions, whereas at low ν's in the kilohertz range there exists a significant discontinuity between the smectic and nematic state. (The T_1 behaviour of the $Cr - S_{A2}$ transition could not be measured with the available field-cycling apparatus because of the poor signal quality for the solid.)

Related effects can be seen by the frequency dependence of T_1, which is presented in Fig. 2 for two temperatures, one in the nematic state (150 °C) and the other in the smectic-A_2 state (136 °C). Both dispersion plots show the $T_1(\nu)$ characteristics known from previous relaxation studies on liquid crystals, namely: (i) a low-frequency plateau, (ii) a strong increase above the kHz range followed by (iii) an intermediate frequency range where the T_1 increase slows down, becoming frequency independent in the smectic-*A* phase, and finally (iv) the development of a second strong dispersion step in the conventional high-frequency NMR regime. But the two plots also indicate rather different details which have not been observed previously with comparable clarity. In particular, range (ii) is much broader and range (iii) is much smaller for the nematic than for the smectic-A_2 mesophase. As a consequence, one finds a crossing point where $T_1[S_{A2}] > T_1[N]$ changes to $T_1[S_{A2}] < T_1[N]$. This means that the process responsible for the range (ii) is better seen in the nematic state, and the process responsible for the range (iii) is more significant in the smectic state! Another, yet minor, distinction is observed at $\nu \simeq 10^4$ Hz, where $T_1[N]$ reveals a "dip", i.e. a slight decrease by about 20% which is not or less clearly visible by $T_1[S_{A2}]$.

In addition to the temperature and frequency dependencies, we also determined the angular dependence of the proton relaxation rate, $1/T_1(\Delta)$, of the S_{A2} sample at high fields by rotating the orientation of the liquid crystal director (perpendicular to the smectic layers) relative to the NMR Zeeman field by an angle Δ. The angular dependence of $1/T_1(\Delta)$ for the S_{A2} phase is very small. It increases only by about 13% when Δ is changed from 0° to 90°. This variation could indicate that the DB5CN sample is only partially oriented in the Zeeman field. However, from the analysis of additional spectra taken at $T = 130\,°C$, for $\Delta = 0°$ and $\Delta = 90°$, it was observed that the sample was well oriented in the magnetic field and could be considered as a monocristal [24]. Related results for the nematic sample are difficult to get because of the fast reorientation of the director axis. However, an indirect way of

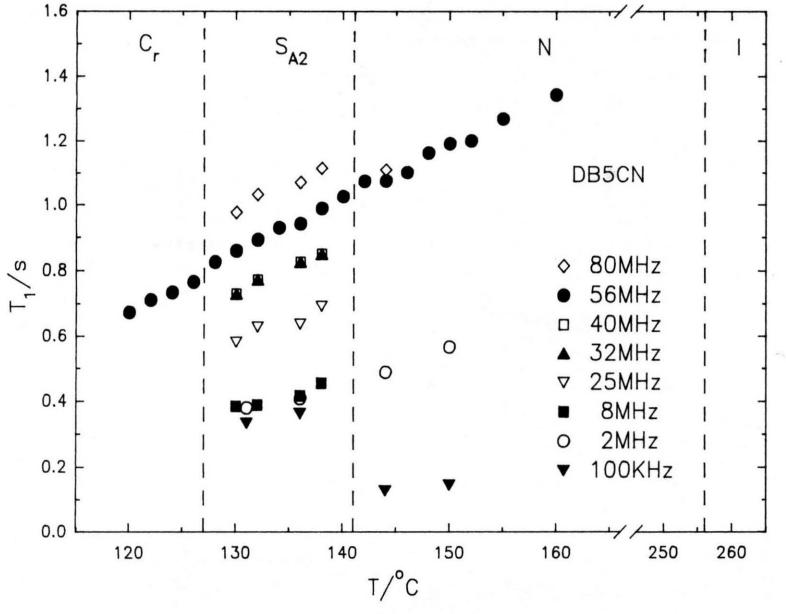

Fig. 1. Temperature dependence of the proton spin relaxation time T_1 of DB5CN at some selected frequencies.

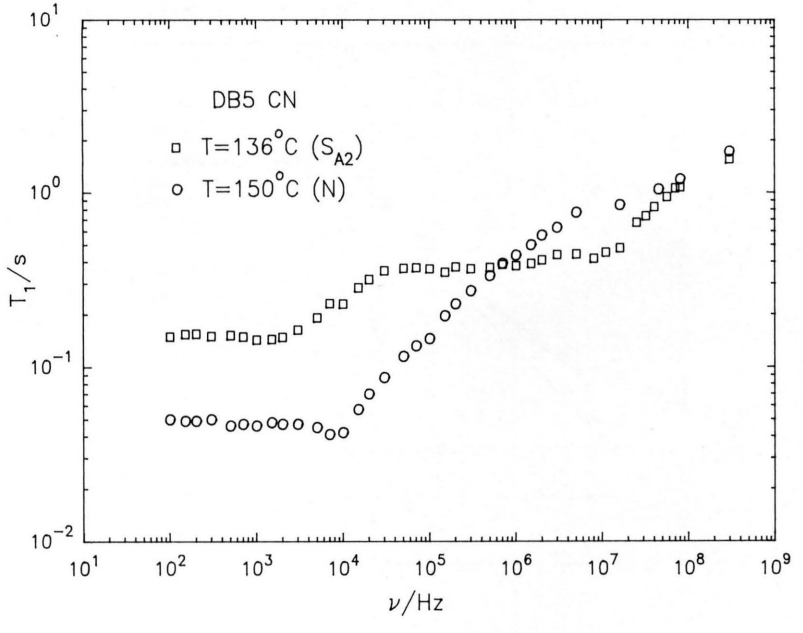

Fig. 2. Frequency dependence of the longitudinal proton relaxation time T_1 of DB5CN at two temperatures, one in the nematic phase (150 °C) the other in the smectic-*A* phase (136 °C).

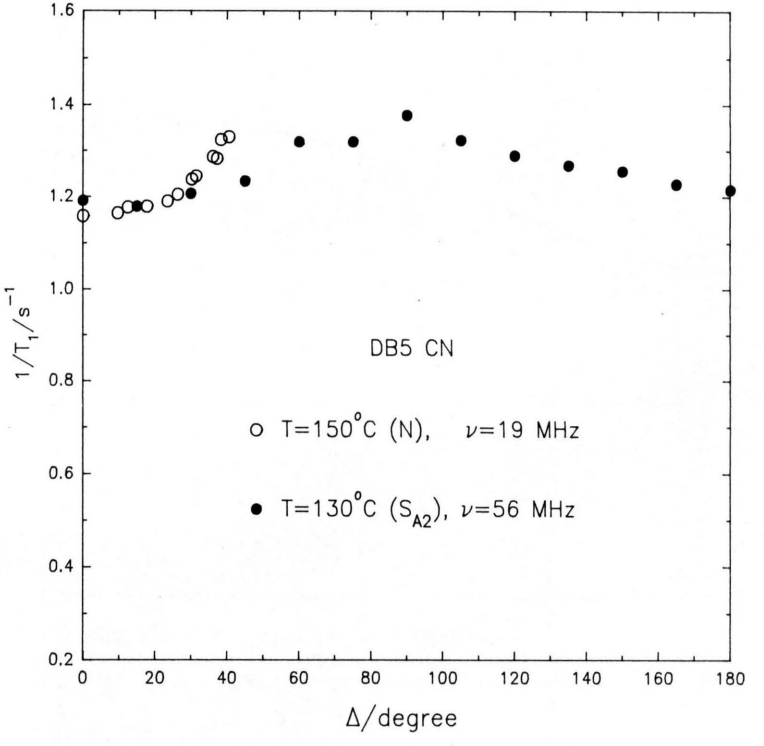

Fig. 3. Angular dependence of the longitudinal proton relaxation rate $1/T_1$ of DB5CN in the smectic-*A* phase for $T = 130$ °C, $\nu = 56$ MHz and in the nematic phase for $T = 150$ °C, $\nu = 19$ MHz.

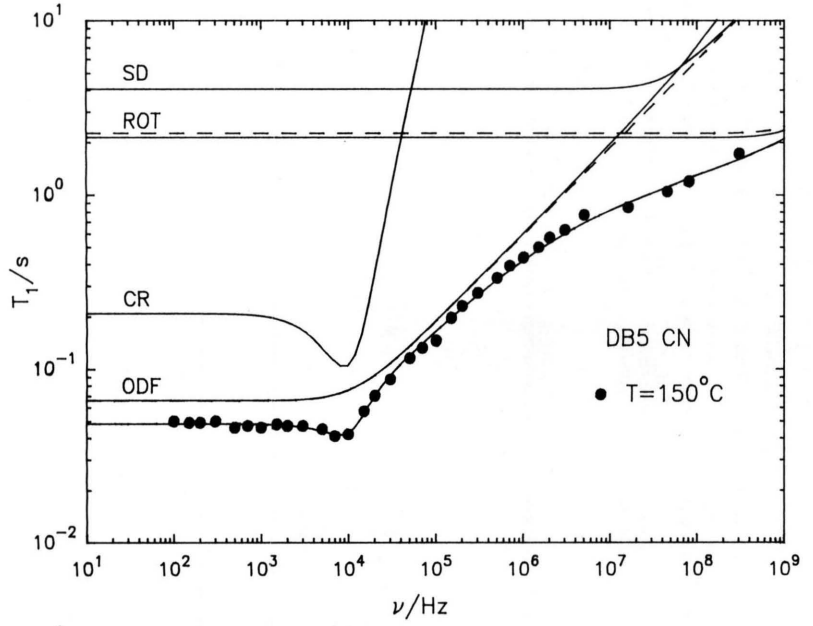

Fig. 4. Fit of the T_1 dispersion data in the nematic phase (150 °C) with the four model contributions Table 1-(1) (nematic case), Table 1-(2) (nematic case), Table 1-(3) and Table 1-(4) (solid lines for $\nu_{C_{max}} \simeq 3.3 \times 10^9$ Hz, dashed lines for $\nu_{C_{max}} \sim \infty$).

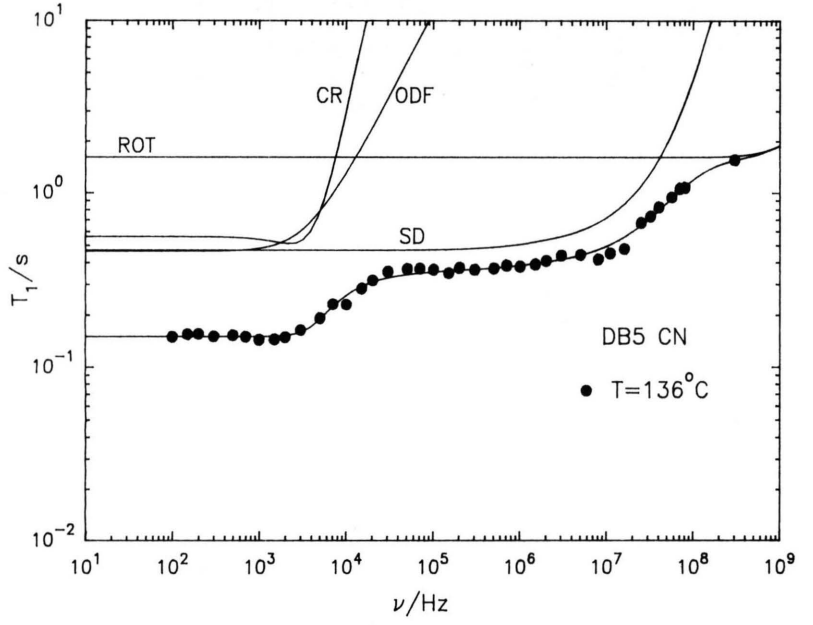

Fig. 6. Fit of the T_1 dispersion data in the smectic-A phase (136 °C) with the four model contributions Table 1-(1) (smectic case), Table (1-(2) (smectic case with $\nu_{C_{max}} \sim \infty$), Table (1-(3) and Table 1-(4).

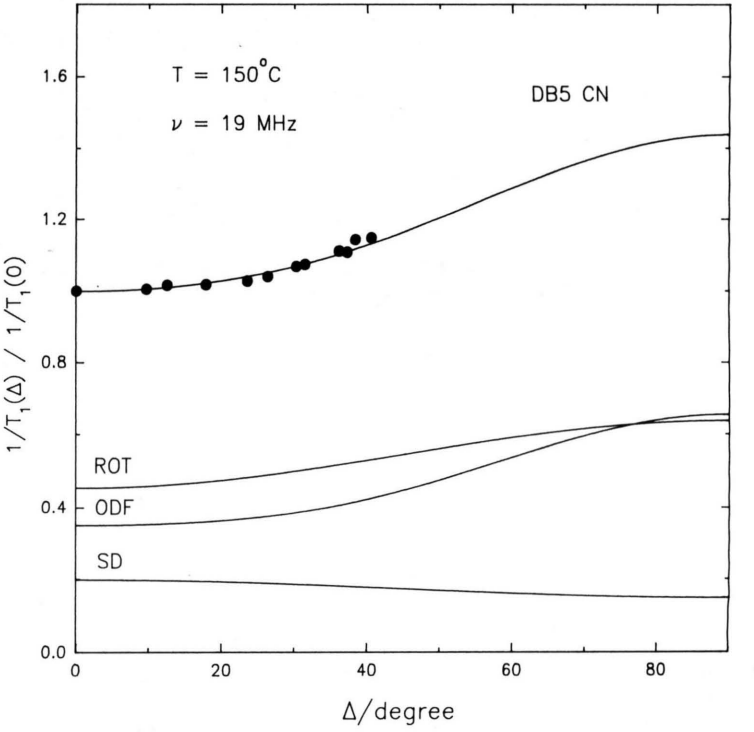

Fig. 5. Fit of the angular dependent $1/T_1$ data in the nematic phase with the model contributions Table 1-(1) (nematic case), and Table 1-(3).

rotating the liquid crystal director with respect to the Zeeman field, is rotating the sample at a steady spinning rate ω_S [25]. In fact, below a critical spinning rate ω_C (which depends on the magnetic field strength) there is a constant dephasing, Δ, between the director and the magnetic field axis. This angle can be obtained from the analysis of the dipolar splitting of the NMR proton spectra. The angular dependence of T_1 can thus be obtained by spinning the sample at different spinning rates. The constraint $\omega_S < \omega_C$ implies that Δ can vary only from 0° to 45°. The T_1's measured with this method were quite reproducible. These data are very important for the interpretation of the relaxation in the nematic phase. The angular results obtained as described above are represented in Fig. 3 for $T =$ 130 °C, $\nu = 56$ MHz (S_{A2} mesophase) and $T = 150$ °C, $\nu = 19$ MHz (nematic mesophase). In addition to the described results, NMR spectra were collected at different temperatures and in both mesophases for the evaluation of the nematic order parameter S (see Table 2).

3. Analysis and Discussion

In order to understand the T_1 relaxation dispersion profiles and their changes between the nematic and smectic samples quantitatively, we tried curve fits with some relaxation models for liquid crystals. It is known from previous studies that proton relaxation measurements – even over a broad frequency range – generally cannot be interpreted unambiguously because of the great number of proton pairs on the liquid crystal molecules and the numerous kinds of molecular motions which may contribute to the average observed relaxation rate. This averaging prevents that the asymptotic dispersion profiles, characteristic of special reorientation processes (e.g. $T_1 \sim \nu^{1/2}$, $T_1 \sim \nu$, $T_1 \sim \nu^{3/2}$ or $T_1 \sim \nu^2$, etc.), fully develop. In the present case, the constraints imposed by the simultaneous analysis of the nematic and smectic phase of the same compound greatly facilitate the model fitting, because the two types of model parameters must be consistent with each other.

Qualitatively, the low and high frequency dispersion profiles shown in Fig. 2 are similar to results reported in the literature for other nematic compounds [3, 4] i.e. they reveal (at least) two relaxation regimes with a low frequency plateau and a high frequency increase. This behaviour was attributed to a superposition of fast non-collective and slow collective molecular reorientations [3], but the details of the *inter*- and *intra*molecular contributions to both mechanisms are still strongly disputed. As a first approach we considered four relaxation mechanisms to interpret the $T_1(\nu)$ data and their changes between the nematic and smectic phase, namely:

1. Translational self-diffusion (SD), first calculated by Vilfan and Žumer for nematics [12] and smectics *A* [13].
2. Order director fluctuations (ODF), originally treated by Pincus [18] and Blinc et al. [19], which for the nematic phase yield, over a broad range, the famous square-root law $T_1 \sim \nu^{1/2}$. For S_A phases one expects either a similar square-root behaviour [19] as in nematics, or a linear dependence $T_1 \sim \nu$, if the order director fluctuations are only due to layer undulations.
3. Local molecular rotations/reorientations (ROT), which can be described by a model which accounts for the rotations along the short and long molecular axis [9]; a more detailed model, which considers both molecular reorientations in the laboratory frame and rotations along the long molecular axis in the molecular frame, proposed by Vold and Vold [17], was also considered.
4. A contribution which takes into account the coupling between proton and nitrogen spins on a molecule; this cross-relaxation process (CR) can become effective if the dipolar proton Zeeman splitting frequency and the quadrupolar nitrogen transition frequencies overlap [21, 26]; this allows a resonant exchange between the two polarizations and thus shortens T_1 at special Larmor frequencies ("quadrupolar dip").

The overall relaxation rate

$$\left(\frac{1}{T_1}\right) = \left(\frac{1}{T_1}\right)_{SD} + \left(\frac{1}{T_1}\right)_{ODF} + \left(\frac{1}{T_1}\right)_{ROT} + \left(\frac{1}{T_1}\right)_{CR}$$

was used to fit the experimental data by a computer assisted least-square method. Table 1 summarizes the explicit expressions of the individual terms and the involved molecular and material model parameters. Note that, for simplicity, potential cross effects between the superimposed mechanisms are not included because the available $T_1(\nu)$ measurements proved to be inadequate to reveal such details. Figures 4–7 illustrate the quality of the final results and the difficulty to distinguish between possible alternatives, in partic-

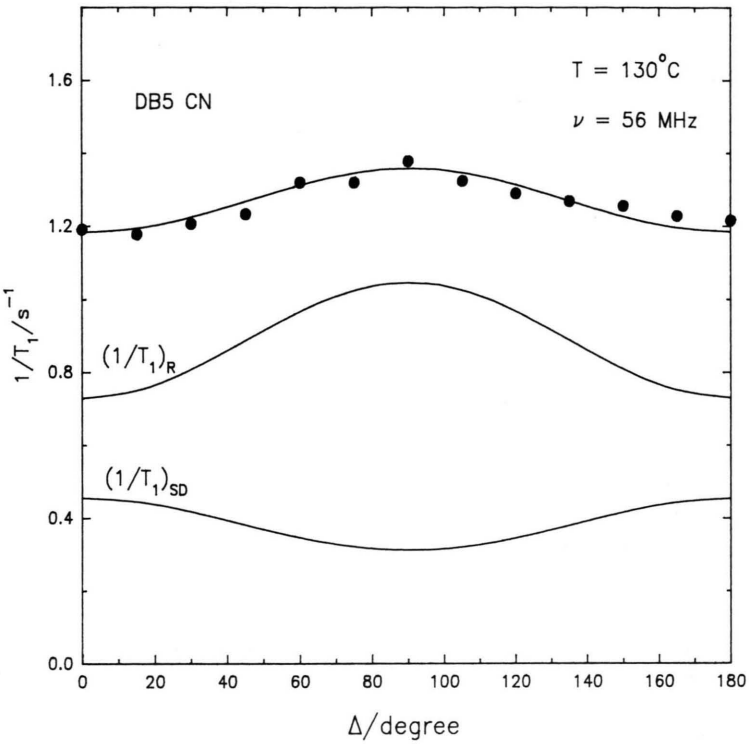

Fig. 7. Fit of the angular dependent $1/T_1$ data in the smectic-A phase with the model contributions Table 1-(1) (smectic case), and Table 1-(3). The contributions coming from the ODF and cross-relaxation mechanisms are negligible at this frequency.

ular with respect to the $T_{1_{ODF}}$ term. According to Table 1, the curve fitting was performed by optimizing up to 10 model parameters: For the self-diffusion term the translational self-diffusion constant ($D_\perp$) perpendicular to the director and the distance of closest approach (d) of two spins belonging to neighboring molecules, or the related jump time $\tau_\perp \equiv d^2/4D_\perp$; for the order director fluctuations the strength (A_N or A_S) of the order director fluctuations contribution and the high and low cut-off frequencies ($\nu_{C_{min}}$, $\nu_{C_{max}}$) of the ODF modes; for the rotational term, described by [9], the rotational correlation time (τ_S) for rotations along the short molecular axis and its ratio to the correlation time along the long molecular axis, τ_S/τ_L; finally for the cross-relaxation term the strength (C), frequency (ν_{CR}) and correlation time (τ_{CR}) of the Lorentz-type cross-relaxation contribution.

Of the remaining model parameters in Table 1, the jump width ratio ($\langle r_\perp^2 \rangle / d^2$), the diffusion anisotropy ($D_\perp/D_\parallel$) and the molecular anisotropy l/d could not be fitted reliably and therefore were estimated from literature results [12, 13, 27]. In particular, l was made equal to the layer spacing of the bilayered S_{A2} phase because molecules diffuse in pairs (dimers) [10, 28] and the density of spins was calculated assuming a bulk density of 10^3 kg m^{-3} for n in Table 2. In addition, the order parameter (S) was estimated from NMR proton measurements, and the geometry factors $A^{(k)}(\alpha_{ij}, r_{ij})$, Table 1, were estimated from the structure of the DB5CN molecules in their most stretched form, Table 2. The averaged elastic constant (K), viscosity (η) and coherence length, (ξ_Z), were obtained from the fitting parameters.

For the nematic mesophase (150 °C), the $T_{1_{ODF}}(\nu)$ square-root law contribution including the low-frequency cut-off and one $T_{1_{CR}}(\nu)$ minimum are well-pronounced in the low frequency dispersion profile, so that the least-squares model fit gives very reliable model parameters. In contrast to this, the assignment of the $T_{1_{SD}}(\nu)$ and $T_{1_R}(\nu)$ terms and the high-frequency cut-off of $T_{1_{ODF}}(\nu)$ is not possible reliably without additional assumptions. We made use of the circumstance that, according to dielectric measurements on other high temperature nematic compounds, the dominating rotational motions about the short axis are so fast that they cause approximately a frequency independent relaxation rate in the considered range (extreme narrowing limit) [14]. Hence the high-frequency dispersion profile must be essentially attributed to the rotations/reorientations process, with minor correc-

Table 1. Theoretical expressions used in the analysis of the experimental data. The procedure and notation are explained in the text.

1. Self-Diffusion (SD) [12, 13]

$$\left(\frac{1}{T_1}\right)_{\mathrm{SD_N}} = \frac{9}{8}\left(\frac{\mu_0}{4\pi}\right)^2 \gamma^4 \hbar^2 \frac{n\tau_\perp}{d^3} Q_N\left(\nu\tau_\perp, \frac{\langle r_\perp^2\rangle}{d^2}, \frac{D_\perp}{D_\parallel}, \frac{l}{d}, \Delta\right),$$

$$\left(\frac{1}{T_1}\right)_{\mathrm{SD_{S_A}}} = \frac{9}{8}\left(\frac{\mu_0}{4\pi}\right)^2 \gamma^4 \hbar^2 \frac{n\tau_\perp}{d^3} Q_{S_A}\left(\nu\tau_\perp, \frac{\langle r_\perp^2\rangle}{d^2}, \frac{D_\perp}{D_\parallel}, \frac{l}{d}, \Delta\right).$$

2. Order Director Fluctuations (ODF) [9, 18, 19, 20]

$$\left(\frac{1}{T_1}\right)_{\mathrm{ODF_N}} = \frac{A_N}{\sqrt{\nu}}\left(g_N\left(\frac{\nu_{C_{max}}}{\nu}\right) - g_N\left(\frac{\nu_{C_{min}}}{\nu}\right)\right),$$

$$g_N(a) = \frac{1}{\pi}\left(\arctan(\sqrt{2a}+1) + \arctan(\sqrt{2a}-1) - \operatorname{arctanh}\left(\frac{\sqrt{2a}}{a+1}\right)\right),$$

$$A_N = \frac{9}{16}\left(\frac{\mu_0}{4\pi}\right)^2 \gamma^4 \hbar^2 \frac{k_B T S^2}{\pi^{3/2}} \frac{\eta^{1/2}}{K^{3/2}} \frac{\overline{(3\cos^2\alpha_{ij}-1)^2}}{4r_{ij}^6} \overline{f_{k1}(\Delta)}^k,$$

$$\nu_{C_{max}} = 1.95^2 \frac{2\pi}{l^2}\frac{K}{\eta}, \quad \nu_{C_{min}} = \frac{2\pi}{\xi_Z^2}\frac{K}{\eta},$$

$$\left(\frac{1}{T_1}\right)_{\mathrm{ODF_{S_A}}} = \frac{A_S}{\nu}\left(\frac{2}{\pi}\arctan\left(\frac{\nu_{C_{max}}}{\nu}\right) - \frac{2}{\pi}\arctan\left(\frac{\nu_{C_{min}}}{\nu}\right)\right),$$

$$A_S = \frac{9}{64}\left(\frac{\mu_0}{4\pi}\right)^2 \gamma^4 \hbar^2 \frac{k_B T S^2}{\pi K_1 \xi_Z} \frac{\overline{(3\cos^2\alpha_{ij}-1)^2}}{4r_{ij}^6} \overline{f_{k1}(\Delta)}^k,$$

$$\nu_{C_{max}} = \frac{2\pi}{d^2}\frac{K_1}{\eta}, \quad \nu_{C_{min}} = \frac{2\pi}{\xi_\perp^2}\frac{K_1}{\eta}.$$

3. Rotations (ROT) [9, 14]

$$\left(\frac{1}{T_1}\right)_{\mathrm{ROT}} = \frac{9}{8}\left(\frac{\mu_0}{4\pi}\right)^2 \gamma^4 \hbar^2 (J^{(1)}(\nu,\Delta) + J^{(2)}(2\nu,\Delta)),$$

$$J^{(k)}(\nu,\Delta) = \frac{4}{3}\sum_{n=0}^{2} f_{kn}(\Delta)\, C_k \sum_{m=0}^{2} \overline{D_{mn}^2 D_{mn}^{2*}}\, A^{(m)} \frac{\tau_m}{1+4\pi^2\nu^2\tau_m^2},$$

$$C_0 = 6, \quad C_1 = 1, \quad C_2 = 4,$$

$$\tau_0 = \tau_S, \quad \frac{1}{\tau_1} = \frac{1}{6\tau_L} + \frac{5}{6\tau_S}, \quad \frac{1}{\tau_2} = \frac{2}{3\tau_L} + \frac{1}{3\tau_S},$$

$$A^{(0)} = \frac{\overline{(3\cos^2\alpha_{ij}-1)^2}}{4r_{ij}^6}; \quad A^{(1)} = \frac{\overline{3\sin^2 2\alpha_{ij}}}{4r_{ij}^6}; \quad A^{(2)} = \frac{\overline{3\sin^4\alpha_{ij}}}{4r_{ij}^6}.$$

The expectation values of the Wigner rotation matrices D_{ij}^2 can be expressed in terms of the nematic order parameter and the expectation value of P_4, $\langle P_4\rangle$, [9, 16]. We assumed that $\langle P_4\rangle \sim \frac{5}{7}S^2$ [32]. The expressions for the angular functions $f_{kn}(\Delta)$ are well known from the literature and can be found in [9] and [12].

4. Cross-Relaxation (CR) [21, 26]

$$\left(\frac{1}{T_1}\right)_{\mathrm{CR}} = \frac{C\tau_{CR}}{1+4\pi^2(\nu_{CR}-\nu)^2\tau_{CR}^2}.$$

Table 2. Fitting parameters obtained for the fits represented in the figures. The notation is explained in the text.

	Fig. 4	Fig. 4, 5	Fig. 6	Fig. 7
$\frac{T}{^\circ C}$	150	150	136	130
$\frac{\tau_\perp \times 10^9}{s}$	0.26	0.26	1.74	1.90
$\frac{D_\perp \times 10^{11}}{m^2\,s^{-1}}$	24.0	24.0	3.59	3.28
$\frac{D_\perp}{D_\parallel}$	0.63	0.63	1	1
$\frac{\nu_{C_{max}} \times 10^{-9}}{Hz}$	∞	3.3	∞	∞
$\frac{\nu_{C_{min}} \times 10^{-3}}{Hz}$	9.9	9.9	2.1	0.2
$\frac{A_N \times 10^{-3}}{s^{-3/2}}$	1.7	1.7	–	–
$\frac{A_S \times 10^{-3}}{s^{-2}}$	–	–	9.0	4.8
$\frac{\tau_S \times 10^{11}}{s}$	5.3	5.6	7.5	8.8
$\frac{C \times 10^{-5}}{s^{-2}}$	4.3	4.3	4.0	0.4
$\frac{\nu_{CR} \times 10^{-3}}{Hz}$	9.1	9.1	3.0	3.0
$\frac{\tau_{CR} \times 10^5}{s}$	2.3	2.3	4.9	4.9
$\frac{\tau_S}{\tau_L}$	4.0	4.0	4.0	4.0
S	0.66	0.66	0.68	0.70

For the remaining parameters we assumed the following values:

$l \simeq 52.5 \times 10^{-10}$ m [10], $d = 5 \times 10^{-10}$ m, $\langle r_\perp^2\rangle/d^2 = 1$, $\nu_{loc} = 2 \times 10^3$ Hz, $n \simeq 3.3 \times 10^{28}$ spins m^{-3}, $A^{(0)} \simeq 7.0 \times 10^{57}$ m^{-6}, $A^{(1)} \simeq 2.7 \times 10^{57}$ m^{-6}, $A^{(2)} \simeq 11.3 \times 10^{57}$ m^{-6}.

tions originating from the other two frequency dependent terms. Figure 4 presents the obtained results under the assumptions of an infinite mode cut-off ($\nu_{C_{max}} \sim \infty$) and with a finite cut-off frequency ($\nu_{C_{max}} = 3.3 \times 10^9$ Hz). Obviously, despite the broad frequency variation the available data do not allow a clear separation of the effects on the dispersion profile caused by the limiting mode ($\nu_{C_{max}}$), the diffusion constants ($D_\perp$, $D_\parallel$) and the ratio between the correlation times τ_S/τ_L, which proves to be important when fitting the angular data. According to Pusiol et al. [21], fine frequency steps in the megahertz regime should also reveal two additional quadrupolar dips due to the proton-nitrogen coupling, but so far the sharpness of the involved energy crossings made them hard do detect [25].

These nematic results are in qualitative agreement with previous proton field-cycling measurements of other high-temperature nematics [3, 4] and deuteron relaxation studies [31]. In particular, the correlation time for rotations of about 10^{-11} to 10^{-10} s is compatible with values obtained for other nematics. Up to about $\nu = 10$ MHz, the general behaviour of the model fit is dominated by the ODF contribution (Table 1-(2)). Only above this range the self-diffusion and rotational mechanisms (Table 1-(1), (3)) become important for the overall relaxation. Their relative importance is limited by the constraints imposed by the smectic data fit; in particular $D_\perp$ and τ_S have to show a physically reasonable temperature behaviour (see Table 2), and so local rotations (Table 1-(3)) seem to be more important than self-diffusion (Table 1-(1)) in this frequency region. This interpretation is confirmed by the curve fit of the T_1 angular data in the nematic phase, Figure 5. The different angular behaviour of $T_{1_R}(\Delta)$ and $T_{1_{SD}}(\Delta)$ doesn't permit an exchange in their relative weights in the curve fit. The value of τ_S/τ_L was made equal to the one obtained from the smectic data fit. Any temperature dependence of τ_S/τ_L is masked by the temperature dependence of the other fitting parameters, namely $D_\perp$, τ_S, and $\nu_{C_{max}}$. The plateau observed in the order director fluctuation dispersion at low frequencies cannot be definitively ascribed to the existence of a low cut-off frequency $\nu_{C_{min}}$, due to a finite coherence length ξ_Z (Table 1-(2)) in the ODF modes; an alternative explanation is possible by taking account of the finite internal local field, which restricts the variation of the locally effective Larmor frequency ($\nu_{eff} = \sqrt{\nu^2 + \nu_{loc}^2}$) [4, 29]. It is expected to distinguish the OF mode and local field models by future deuteron field-cycling studies [4]. The values of the averaged elastic constant K, effective viscosity η and coherence length ξ_Z, were obtained from the fitting parameters A_N, A_S, $\nu_{C_{max}}$ and $\nu_{C_{min}}$ ($K \sim 10^{-11}$ N, $\eta \sim 10^{-3}$ kg m^{-1} s^{-1}, $\xi_Z \sim 10^{-6}$ m). It should be noted that, with exception of the order director fluctuations' weight for the nematic phase, A_N, A_S, $\nu_{C_{max}}$, and $\nu_{C_{min}}$ are highly correlated with other fitting parameters, and therefore their values are not unique.

For the DB5CN smectic phase (136 °C), the difficulties to analyze the dispersion profile are rather different. In this case the $T_{1_{ODF}}(\nu)$ dispersion step is rather narrow, so that it could be described both by a square-root law $T_1 \sim \nu^{1/2}$ [13] together with an unusually low upper cut-off frequency ($\nu_{C_{max}}$ near 10^5 Hz), and also by a linear profile $T_1 \sim \nu^1$ [19] without the necessity to take into account a finite cut-off limit, giving both the same good curve fits in the low frequency range. However, the elastic constant K_{S_A}, which in the smectic phase should be essentially K_1 (K_2 and K_3 diverge) [30] and the effective viscosity η_{S_A} obtained from the curve fit with $T_1 \sim \nu^{1/2}$ are unreasonable high ($K_{S_A} \sim 10^{-8}$ N and $\eta_{S_A} \sim 10^5$ kg m^{-1} s^{-1}) when the value of K_1 should not be very different from the one in the nematic phase [31]. Therefore, for the present we think that layer undulations [19] are the more reasonable collective motion which is responsible for the $T_{1_{ODF}}$ relaxation process. Figure 6 presents the best fit using the linear law for $T_{1_{ODF}} \sim \nu^1$ in the curve fit.

Surprisingly, in the smectic fits the additional proton-nitrogen cross coupling is a negligible contribution to the overall dispersion profile since the quadrupolar dips are absent or at least less evident than in the nematic phase. In contrast to this, the self-diffusion contribution is the dominant mechanism for frequencies above 50 kHz. Similar changes related to the nematic-to-smectic-A phase transition are known for other smectic-A and partially bilayered smectic-A mesogens [7–9, 21]; they essentially reflect the strong decrease of the diffusion constant at lower temperatures. The self-diffusion coefficients obtained in both mesophases are in agreement with reported results for other liquid crystals with similar mesophases [27].

A combined analysis of the angle dependent data in the smectic phase (130 °C) presented in Fig. 3 with the frequency dependent data shown in Fig. 2 confirms that above 40 MHz the rotational process becomes more important than self-diffusion as illustrated by the model fit of Figure 7. The observed angular depen-

dence is well fitted with a superposition of a large contribution from the rotational mechanism and a small self-diffusion contribution (Table 1-(1)), which involves a $1/T_1(\Delta)$ variation opposite to the observed one. The contribution of the ODF mechanism is negligible at this frequency.

The use of a more detailed model to describe the rotations/reorientations mechanism such as the one proposed by Vold and Vold [17] was also considered. The curve fits obtained when including this model in the overall relaxation theoretical expression were quite similar to the ones presented in Figs. 4–7. However, due to the increase of degrees of freedom in the parameter space introduced by this model many good fits could be obtained with different sets of parameters, all of them with very similar contributions from the rotation/reorientations mechanism. For a typical fit in the smectic phase, assuming a strong collision rotational process, the correlation times for reorientations of the molecules along the short and long molecular axis were of the order ot 10^{-10} s and for rotations of a molecule along its long molecular axis (γ motion [17]) the correlation time was of the order 10^{-11} s. These values are in agreement with the corresponding ones presented in Table 2, considering the simplified model used in those fits, and agree with others recently reported for deuteron relaxation studies [31].

4. Conclusions

In this paper we present a proton spin-lattice relaxation study in the nematic and smectic A_2 mesophases of the compound DB5CN. The dispersion behaviour of the relaxation time T_1 is for frequencies between 10 kHz and 10 MHz rather different in these mesophases. The T_1 plateau observed in the smectic A_2 phase over a broad intermediate frequency range is not present in the nematic phase and could only be interpreted in terms of a more important self-diffusion contribution at these frequencies. The angle dependent $1/T_1$ data, which increase with the angle in both mesophases, at fixed frequencies, permit to distinguish the relative importance of the relaxation contributions coming from rotations and self-diffusion since each mechanism has a particular signature with respect to this dependence. A consistent T_1 data analysis of both phases in view of the available theoretical models for the relaxation mechanisms expected for this kind of mesophases, makes possible to conclude that in the nematic phase the most relevant mechanisms are the order director fluctuations and the rotation/reorientation mechanisms. In the smectic phase the most important ones are self-diffusion and rotations/reorientations. The collective molecular motions are order director fluctuations in the nematic case, where they are described by the usual square root law, $T_1 \sim \nu^{1/2}$, and are layer undulations in the smectic case with the linear law $T_1 \sim \nu$. The relative contributions of self-diffusion and rotations/reorientations cannot be exchanged. The rotational correlation times are of the order of 10^{-10}–10^{-11} s, as previously reported [7, 9] for other compounds, but their absolute values depend on the particular model used to fit the data. Both models used for this relaxation mechanism gave good fits with the same conclusions. From the fitting parameters some viscoelastic parameters were obtained. In both mesophases the inclusion of a cross-relaxation mechanism between protons and nitrogens could improve the relaxation dispersion fits at low frequencies.

Acknowledgements

The authors acknowledge the financial support of JNICT (Project 87/470), thank Dr. Helena Santos (Centro de Química Estrutural – INIC) for the experimental help with the Bruker CXP Spectrometer, and Dr. J. Figueirinhas for scientific discussions. In particular, P. J. Sebastião also thanks Dr. K.-H. Schweikert, Dipl. Phys. R. Humpfer, A Rudnicki, and J. Mager for their helpful discussions about the experimental procedures of fast NMR field-cycling, and finally the DAAD for a fellowship.

[1] R. L. Vold and R. R. Vold, Nuclear Magnetic Relaxation in Liquid Crystals, edited by J. W. Emsley, Reidel Publ. Dordrecht 1983.
[2] P. de Gennes, The Physics of Liquid Crystals, Clarendon Press, Oxford 1974.
[3] F. Noack, M. Notter, and W. Weiß, Liq. Cryst. **3,** 907 (1988).
[4] F. Noack and K. H. Schweikert, in press, The Molecular Dynamics of Liquid Crystals, edited by G. R. Luckhurst, Kluver Acad. Publ., Dordrecht.
[5] F. Hardouin, A. M. Levelut, M. F. Achard, and G. Sigaud, J. Chimie Physique **80,** 53 (1983).
[6] G. Sigaud, F. Hardouin, M. F. Archard, and A. M. Levelut, J. Physique **42,** 107 (1981).
[7] A. C. Ribeiro, P. J. Sebastião, and M. Vilfan, Liq. Cryst. **3,** 937 (1988).
[8] K. H. Schweikert and F. Noack, Z. Naturforsch. **44a,** 597 (1989).
[9] P. J. Sebastião, A. C. Ribeiro, M. H. Godinho, D. Guillon, and M. Vilfan, Liq. Cryst. **11,** 621 (1992).
[10] F. Hardouin, A. M. Levelut, J. J. Banattar, and G. Sigaud, Sol. State. Commun. **33,** 337 (1980).
[11] H. C. Torrey, Phys. Rev. **92,** 962 (1953).
[12] S. Žumer and M. Vilfan, Phys. Rev. **A17,** 427 (1978).
[13] M. Vilfan and S. Žumer, Phys. Rev. **A21,** 672 (1980).
[14] A. Abragam, The Principles of Nuclear Magnetism, Clarendon Press, Oxford 1962.
[15] P. L. Nordio, G. Rigatti, and U. Segre, J. Chem. Phys. **56,** 2117 (1972).
[16] P. A. Beckmann, J. W. Emsley, G. R. Luckhurst, and D. L. Tuma, Mol. Phys. **59,** 97 (1986).
[17] R. L. Vold and R. R. Vold, J. Chem. Phys. **88,** 1443 (1988).
[18] P. Pincus, Sol. State Commun. **7,** 415 (1969).
[19] R. Blinc, M. Luzar, M. Vilfan, and M. I. Burgar, J. Chem. Phys. **63,** 3445 (1975).
[20] M. Vilfan, M. Kogoj, and R. Blinc, J. Chem. Phys. **86,** 1055 (1987).
[21] D. Pusiol and F. Noack, Liq. Cryst. **5,** 377 (1989).
[22] H. Bender, F. Noack, M. Vilfan, and R. Blinc, Liq. Cryst. **5,** 1233 (1989).
[23] F Noack, Progr. Nucl. Magn. Resonance Spectroscopy **18,** 171 (1986).
[24] P. J. Sebastião, A. C. Ribeiro, H. T. Nguyen, and F. Noack, unpublished results.
[25] H. Gasparoux and J. Prost, J. Physique **32,** 953 (1971).
[26] F. Winter and R. Kimmich, Mol. Phys. **45,** 3 (1982).
[27] G. J. Krüger, Physics Reports (Rev. Section Phys. Lett.) **82,** 229 (1982).
[28] D. Guillon and A. Skoulios, J. Physique **45,** 607 (1984).
[29] D. Wolf, Spin-Temperature and Nuclear-Spin Relaxation in Matter, Basic Principles and Applications, Oxford Univ. Press, London, 1979.
[30] W. H. de Jeu, Physical Properties of Liquid Crystalline Materials, Gordon and Breach, Science Publishers Inc., London 1980.
[31] J. M. Goetz, G. L. Hoatson, and R. L. Vold, J. Chem. Phys. **97,** 1306 (1992).
[32] U. Fabbri and C. Zannoni, Mol. Phys. **58,** 763 (1986).